Supplementary information

In-situ Synthesis of Fe_2O_3 Nanospheres/Co_3O_4 Nanowires-Connected Reduced Graphene Oxide Hybrid Networks for High-Performance Supercapacitor

Yan Wang,*[a,b] Jianhao Zhou,[a] Zhiyu Zhou,[a] Huifang Lv,[a] Bingni Gu,[c,d,e] Kuangye Wang, [c,d,e] Zexiang Chen,*[, a,b] Xinyu Yan,[a] Jijun Zhang,[a] Wen-Wu Liu,[f] and Yu-Lun Chueh*[, c,d,e]

[a] *School of Optoelectronic Science and Engineering of UESTC, University of Electronic Science and Technology of China, Jianshe North Road 4, 610054 Chengdu, China*

[b] *Sichuan Province Key Laboratory of Display Science and Technology, Jianshe North Road 4, 610054 Chengdu, China*

[c] *Department of Materials Science and Engineering, National Tsing Hua University, Hsinchu, 30013, Taiwan.*

[d] *Frontier Research Center on Fundamental and Applied Sciences of Matters, Hsinchu, 30013, National Tsing Hua University, Hsinchu 30013, Taiwan*

[e] *Department of Physics, National Sun Yat-Sen University, Kaohsiung, 80424, Taiwan.*

[f] *State Key Laboratory of Advanced Processing and Recycling of Nonferrous Metals, Lanzhou University of Technology, Lanzhou 730050, PR China*

**E–mail: wangyan127@uestc.edu.cn (Y. Wang); zxchen@uestc.edu.cn (Z. X. Chen) and ylchueh@mx.nthu.edu.tw (Y. L. Chueh)*

Table S1

comparison of energy density, power density or specific capacitance of RGO-based composites

Material	Capacitance ($F \cdot g^{-1}$)	Energy density($Wh \cdot kg^{-1}$)	Power density($kW \cdot kg^{-1}$)
Fe-Co-S/GNF	**850**	**——**	**——**
Mn-Zn-Fe-O/G-ink	**——**	**75.65**	**6.6**
RGO/Mn_3O_4	**194.8**	**——**	**——**
Fe_3O_4@PGNs	**312-892**	**——**	**——**
Fe_2O_3/rGO	**522**	**——**	**——**
This work	**784**	**70.78**	**9.94**

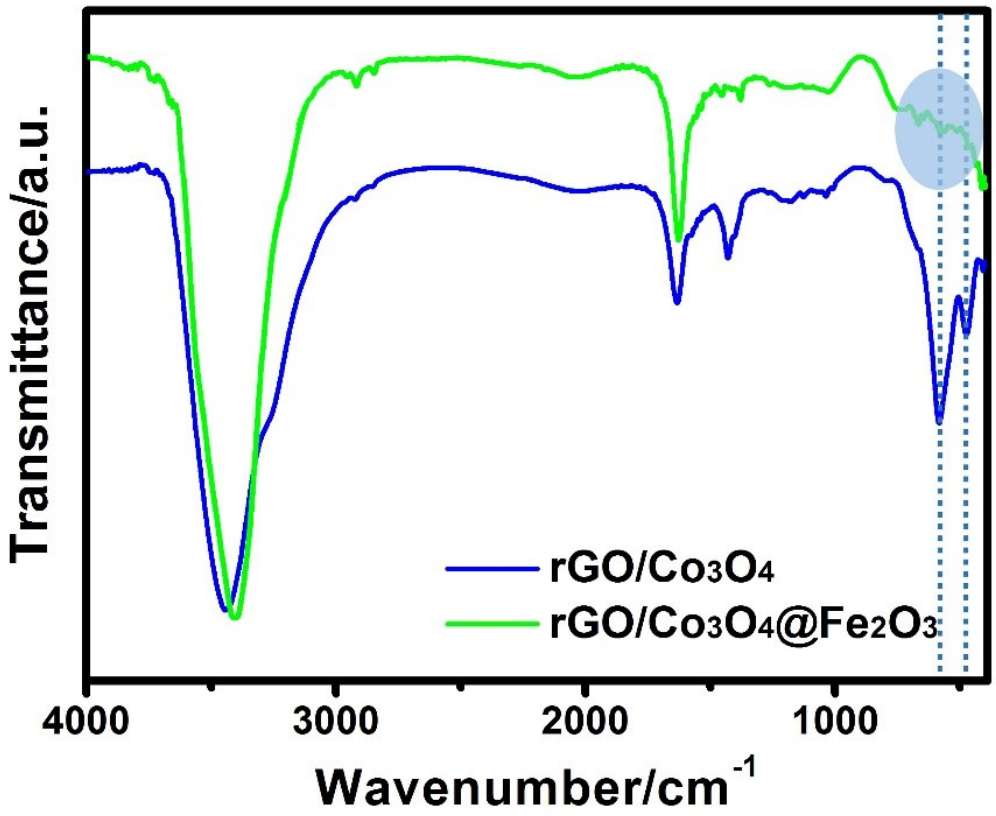

Figure S1 Fourier transform infrared spectroscopy (FTIR) spectra of rGO/Co_3O_4 and rGO/Co_3O_4@Fe_2O_3 samples.

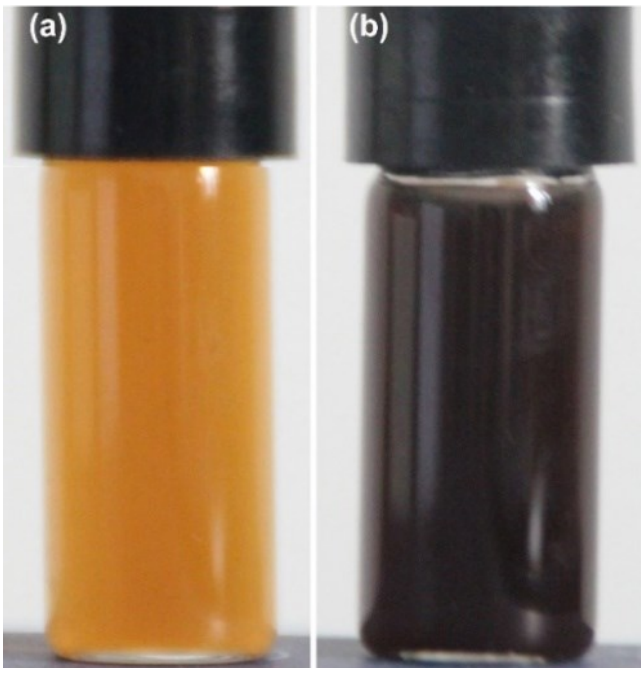

Figure S2 Photographs of (a) GO suspensions and (b)PSS-modified rGO.

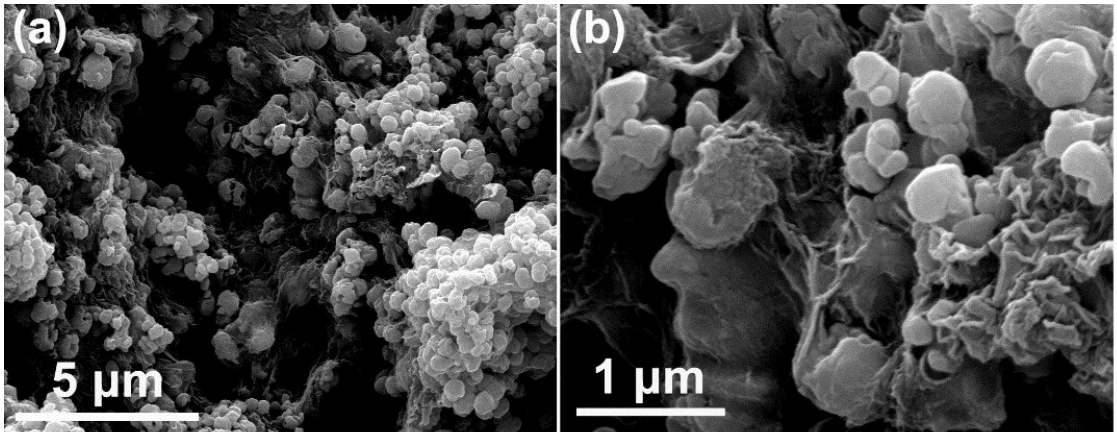

Figure S3 (a) Low- and (b) high-magnification SEM images of rGO/Fe_2O_3 NSs prepared with the similar method.

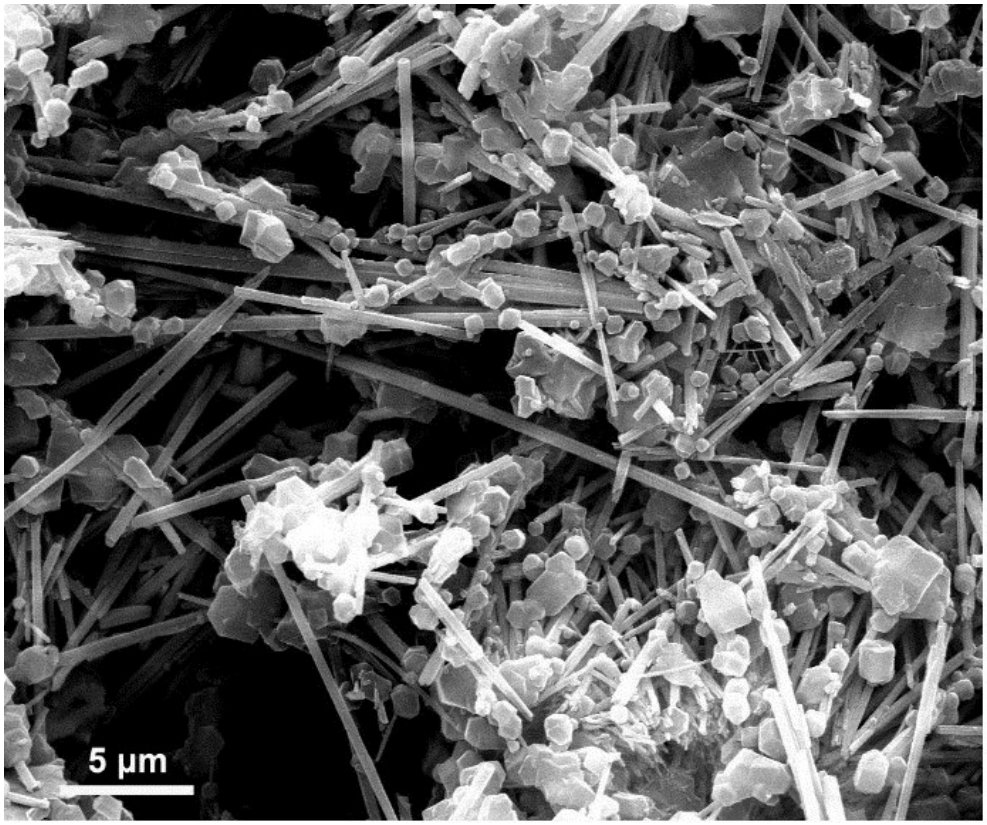

Figure S4 SEM images of Co_3O_4/Fe_2O_3 prepared without rGO by the similar method.

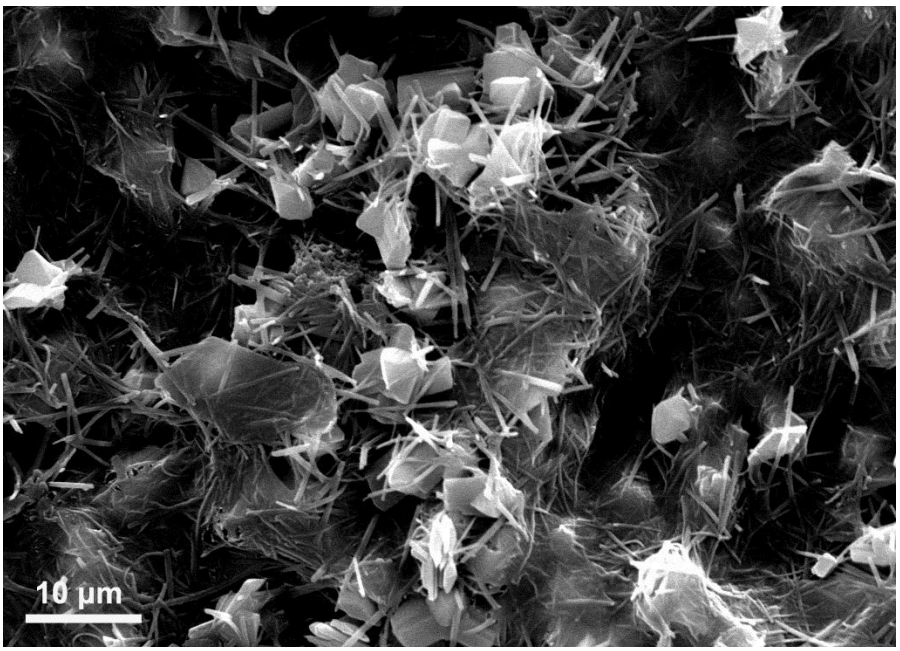

Figure S5 SEM images of Mixture (physical mixture of rGO, Co_3O_4 and Fe_2O_3).

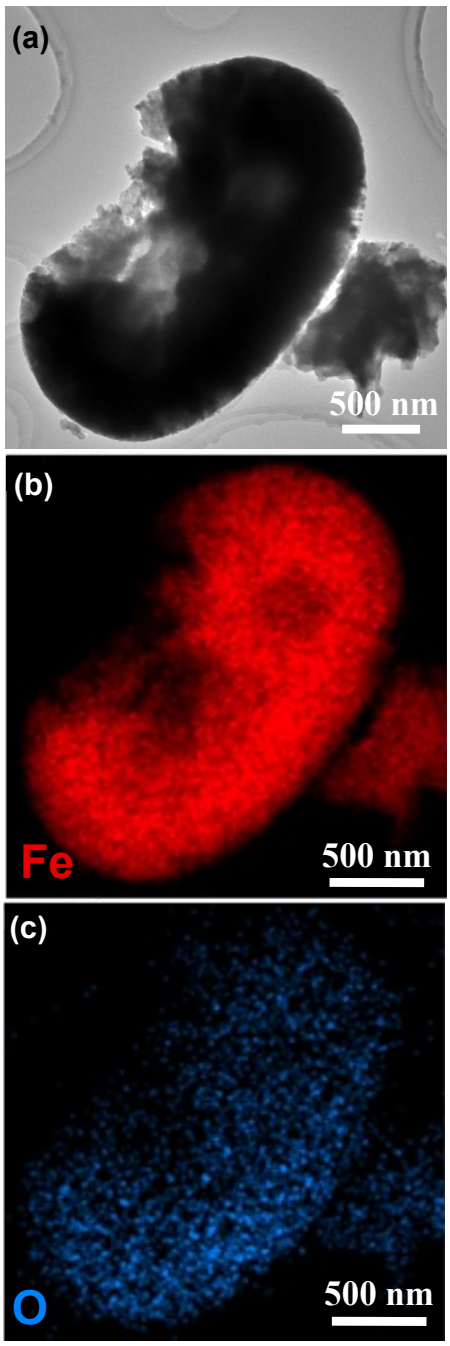

Figure S6 (a)–(c) EDS mapping images of Fe and O from a Fe_2O_3 NS.

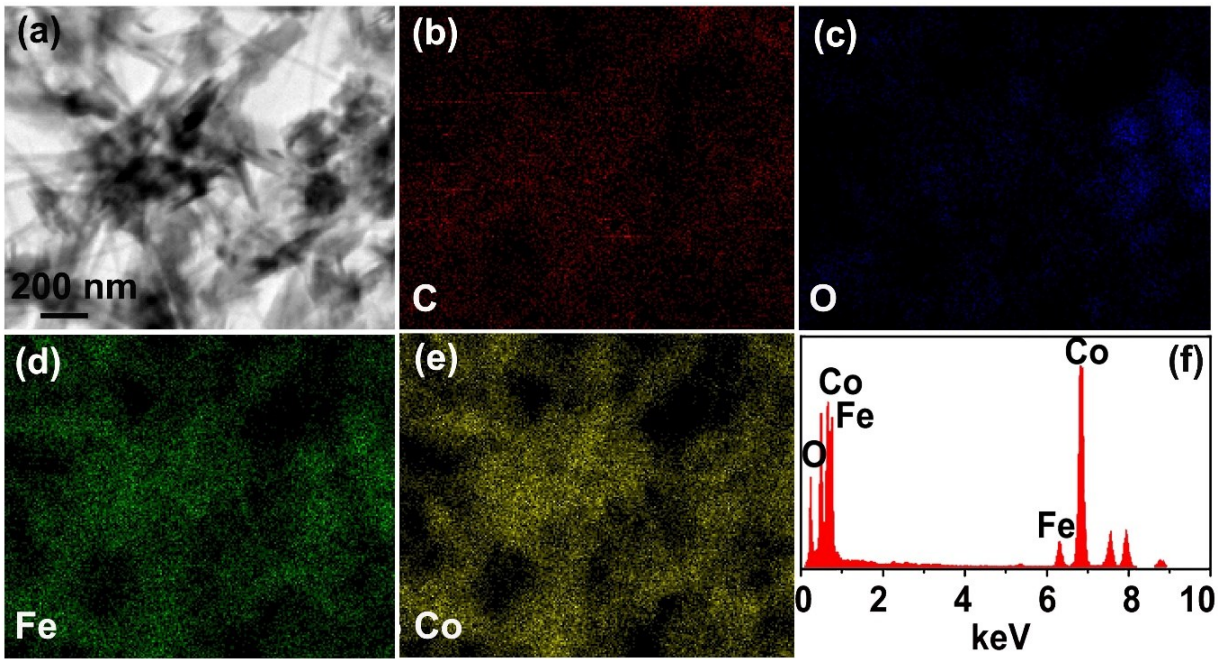

Figure S7 (a)–(e) EDS mapping images of C, O, Fe and Co from the rGO/Co_3O_4@Fe_2O_3 hybrid networks. (f) EDS spectra of rGO/Co_3O_4@Fe_2O_3 hybrid networks.

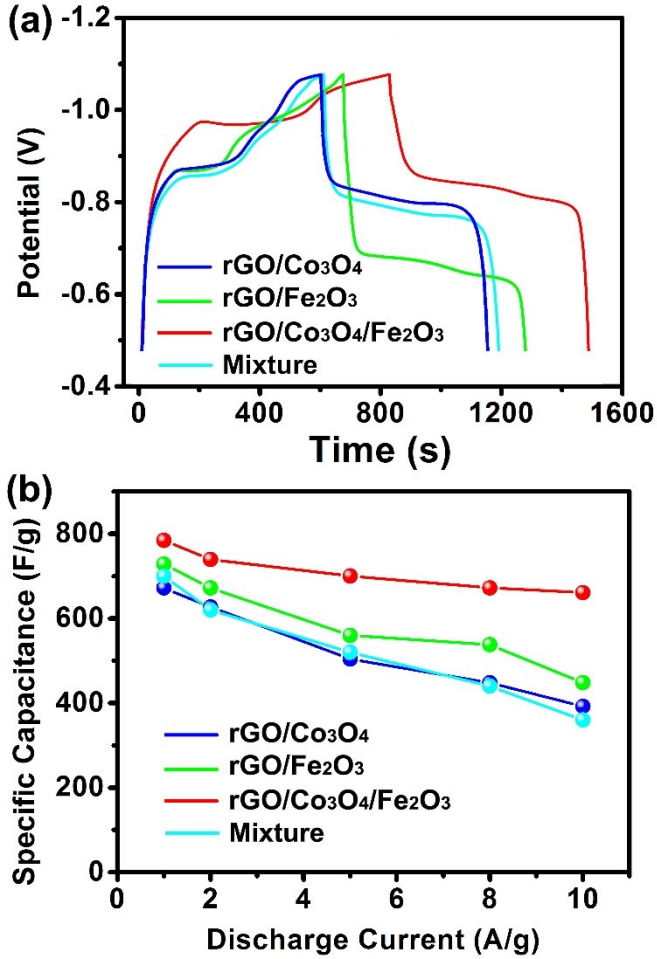

Figure S8 (a) Charge-Discharge curves of the rGO/Co_3O_4 NWs, rGO/Fe_2O_3 NSs the Mixture and rGO/Co_3O_4@Fe_2O_3 hybrid networks at 1 $A \cdot g^{-1}$. (b) Rating performance of rGO/Co_3O_4 NWs, rGO/Fe_2O_3 NSs the Mixture and rGO/Co_3O_4@Fe_2O_3 hybrid networks at various discharge current.

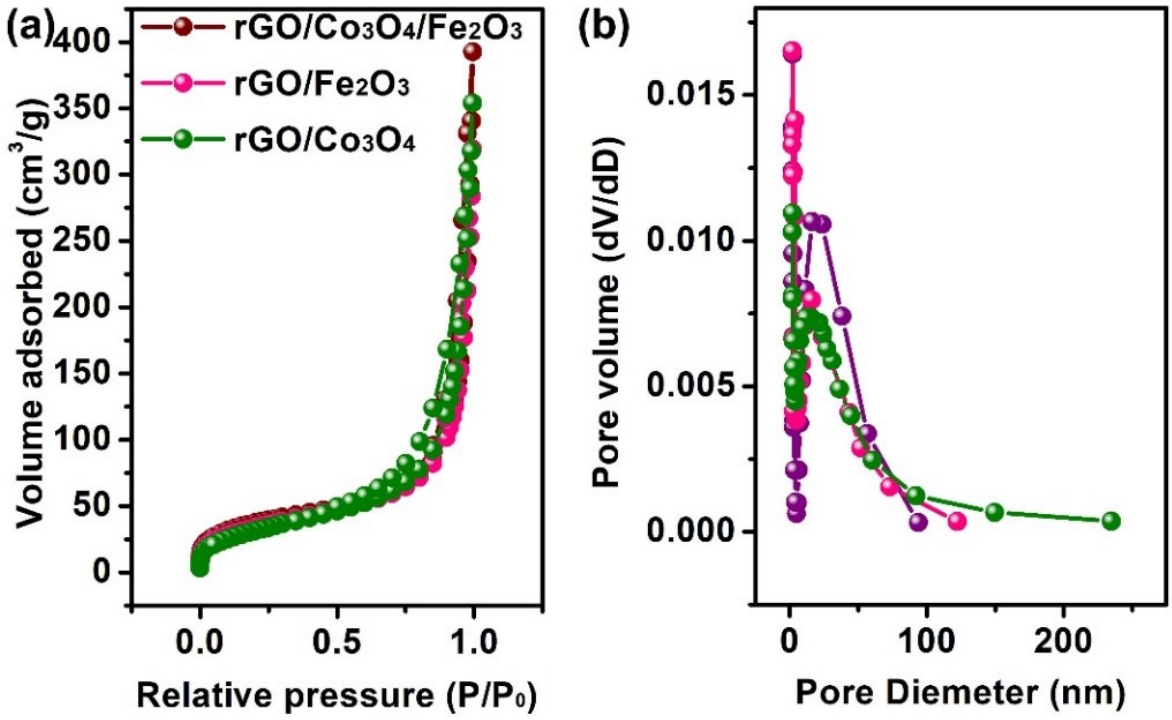

Figure S9 The Brunauer–Emmett–Teller (BET) surface areas and the pore size distribution of the three samples were tested. (a)The surface area of rGO/Co_3O_4@Fe_2O_3 hybrid networks is 165 $m^2 \cdot g^{-1}$, which is larger than that of either (b) rGO/Co_3O_4 NWs or rGO/Fe_2O_3 NSs.

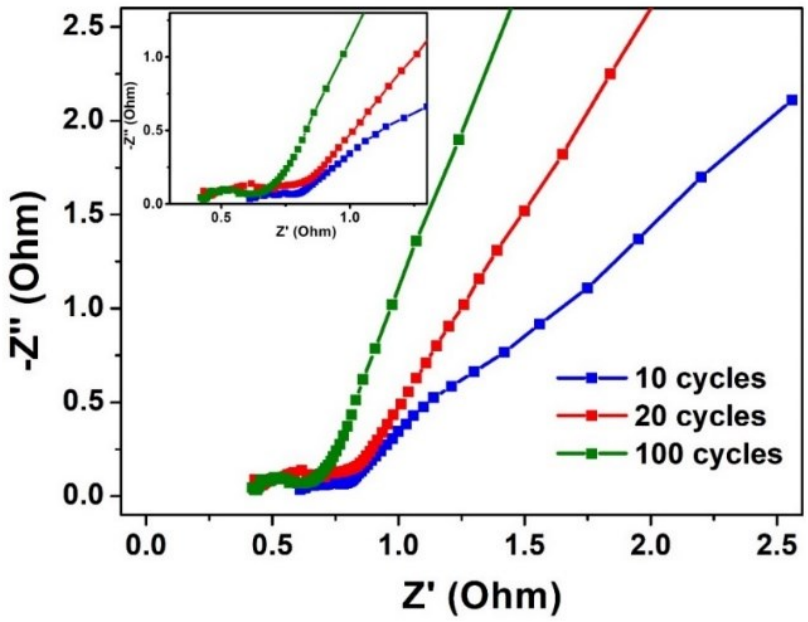

Figure S10 The comparison of the complex plane impedance plots (Nyquist plots) of rGO/Co_3O_4@Fe_2O_3 hybrid networks at different cycles.

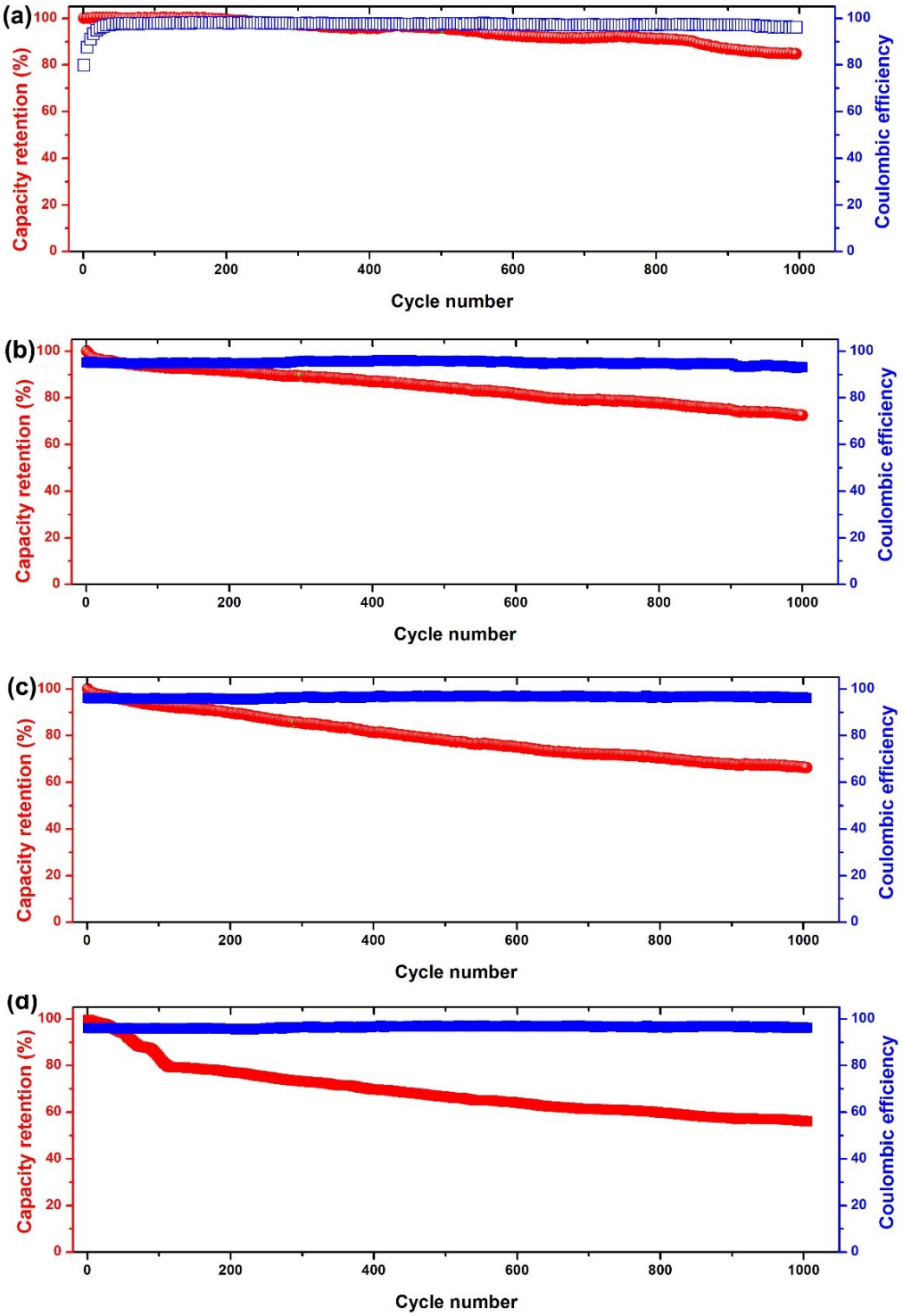

Figure S11 Cycling testes of (a) NiAl–LDH//rGO/Co_3O_4@Fe_2O_3, (b) NiAl–LDH//rGO/Co_3O_4 and (c) NiAl–LDH//rGO/Fe_2O_3 (d) NiAl–LDH//Mixture devices at a current density of 1.0 $A \cdot g^{-1}$ and the corresponding Coulombic efficiency of the devices.